

Electronic Supplementary Information

An Oxygen Vacancies-Rich Two-Dimensional Au/TiO₂ Hybrid for Synergistically Enhanced Electrochemical N₂ Activation and Reduction

Sen Zhao⁺, Han-xuan Liu⁺, Yu Qiu, Shuang-quan Liu, Jin-xiang Diao, Chun-ran Chang,* Rui Si, Xiao-hui Guo*

Corresponding email: guoxh2009@nwu.edu.cn, changer@mail.xjtu.edu.cn
Tel (Fax): (+)86-29-81535025.

⁺ These authors contributed equally to the work.

Details of DFT calculations

All the calculations were performed using the Vienna Ab-initio Simulation Package (VASP).^[1] A plane-wave basis set with an energy cutoff of 400 eV was used to treat the valence electrons. The projected-augmented wave (PAW) pseudopotentials were used to describe the core electrons^[2] and the DFT+ U ^[3] ($U = 5.0$ eV) method was utilized for the $3d$ orbital of Ti in TiO_2 . The generalized gradient approximation (GGA) method with Perdew-Burke-Ernzerh of (PBE) functional for the exchange-correlation term was used^[4]. The Brillouin zone sampled with $3 \times 3 \times 1$ and $7 \times 7 \times 1$ Monkhorst-Pack grids were adopted for reaction thermodynamics and density of states (DOS) calculations, respectively.^[5] The solvation effect was not considered in the calculations as the energy deviations in NRR is within 0.1 eV.^[6] The energies of reaction species were obtained as $\Delta E = \Delta E_{\text{total}} + \Delta E_{\text{ZPE}} - U \cdot n e$,^[7, 8] where ΔE_{total} is the total energy calculated from DFT calculations, ΔE_{ZPE} is the zero-point energy, U is the potential for electrochemistry process, n is the number of electrons participated in the step, and e is the elementary charge. Reversible hydrogen electrode (RHE) was taken as the benchmark of potential in these calculations for adjusting the total energy of hydrogen ion to 1/2 energy of H_2 .^[8] The thermodynamic data of H_2 , N_2 and NH_3 were obtained from NIST.^[9] The values of band centers were obtained from $E_{\text{band center}} = E_{\text{PDOS total}} / I$,^[10] where $E_{\text{PDOS total}}$ is the integral of the product of DOS and energy, I is the integral of DOS. The interval from -25 eV to 5 eV were used for calculating the d band center, the interval below the Fermi level were used for calculating the valence band center, and the interval above the Fermi level were used for calculating the conduction band center.

The catalyst model was built based on the mainly exposed $\text{TiO}_2(112)$ surface which was identified as the substrate of Au_6 clusters from HRTEM. The constructed $\text{TiO}_2(112)$ slab contains four atomic layers with two bottom atomic layers constrained during relaxation. A vacuum space of 10 Å thick was used to avoid the interaction between surface slabs. An Au_6 cluster having two atomic layers was set on the $p(2\times 2)$ $\text{TiO}_2(112)$ surface as the initial catalyst structure. After relaxation, the Au_6 cluster become flat on the surface, reflecting the extensibility of gold.

References:

- [1] a) G. Kresse, J. Hafner, *Phys. Rev. B* **1993**, *47*, 558; b) G. Kresse, J. Hafner, *Phys. Rev.B* **1994**, *49*, 14251; c) G. Kresse, J. Furthmüller, *Comput. Mater. Sci.* **1996**, *6*, 15.
- [2] a) P. E. Blöchl, *Phys. Rev. B* **1994**, *50*, 17953; b) G. Kresse, D. Joubert, *Phys. Rev. B* **1999**, *59*, 1758.
- [3] S.L.Dudarev,G.A.Botton,S.Y.Savrasov,C.J.Humphreys,A.P.Sutton,*Phys.Rev.B.* **1998**, *57*, 1505.
- [4] J. P. Perdew, K. Burke, M. Ernzerhof, *Phys. Rev. Lett.* **1996**, *77*, 3865.
- [5] H. J. Monkhorst, J. D. Pack, *Phys. Rev. B* **1976**, *13*, 5188.
- [6] J. H. Montoya, C. Tsai, A. Vojvodic, J. K. Nørskov, *ChemSusChem* **2015**, *8*, 2180.
- [7] Y. F. Fang, Z. C. Liu, J. R. Han, Z. Y. Jin, Y. Q. Han, F. X. Wang, Y. S. Niu, Y. P. Wu, Y. H. Xu, *Adv. Energy Mater.* **2019**, 1803406
- [8] J. Rossmeisl, Z. W. Qu, H. Zhu, G. J. Kroes, J. K. Nørskov, *J. Electroanal. Chem.* **2007**, *607*, 83.
- [9] <http://cccbdb.nist.gov/>
- [10] a) J. R. Kitchin, J. K. Nørskov, M. A. Bartheau, J. G. Chen, *J. Chem. Phys.* **2004**, *120*, 10240; b) L. Bai, X. Wang, Q. Chen, Y. Ye, H. Zheng, J. Guo, Y. Yin, C. Gao, *Angew. Chem.-Int. Edit.* **2016**, *55*, 15656.

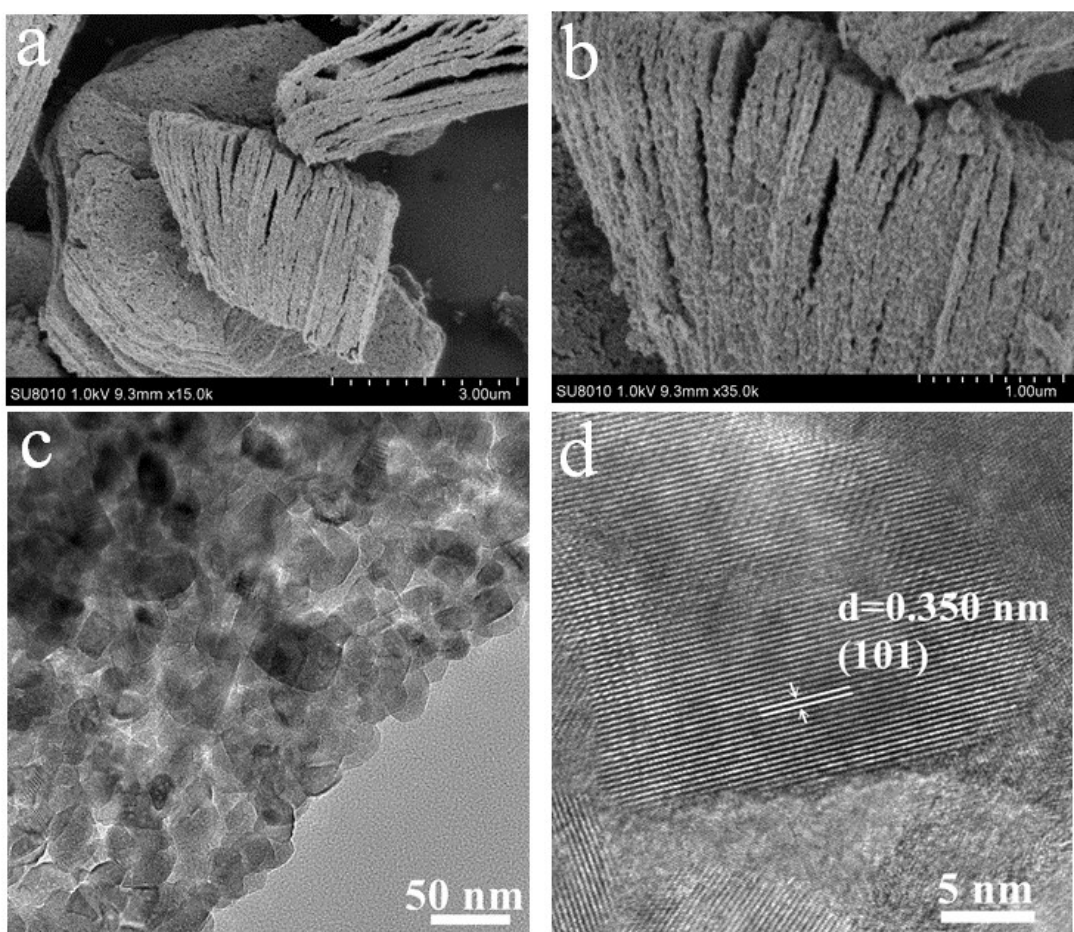


Figure S1: Morphology and structure analysis for pure TiO_2 sample, (a-b) SEM images; (c-d) TEM images with different magnifications.

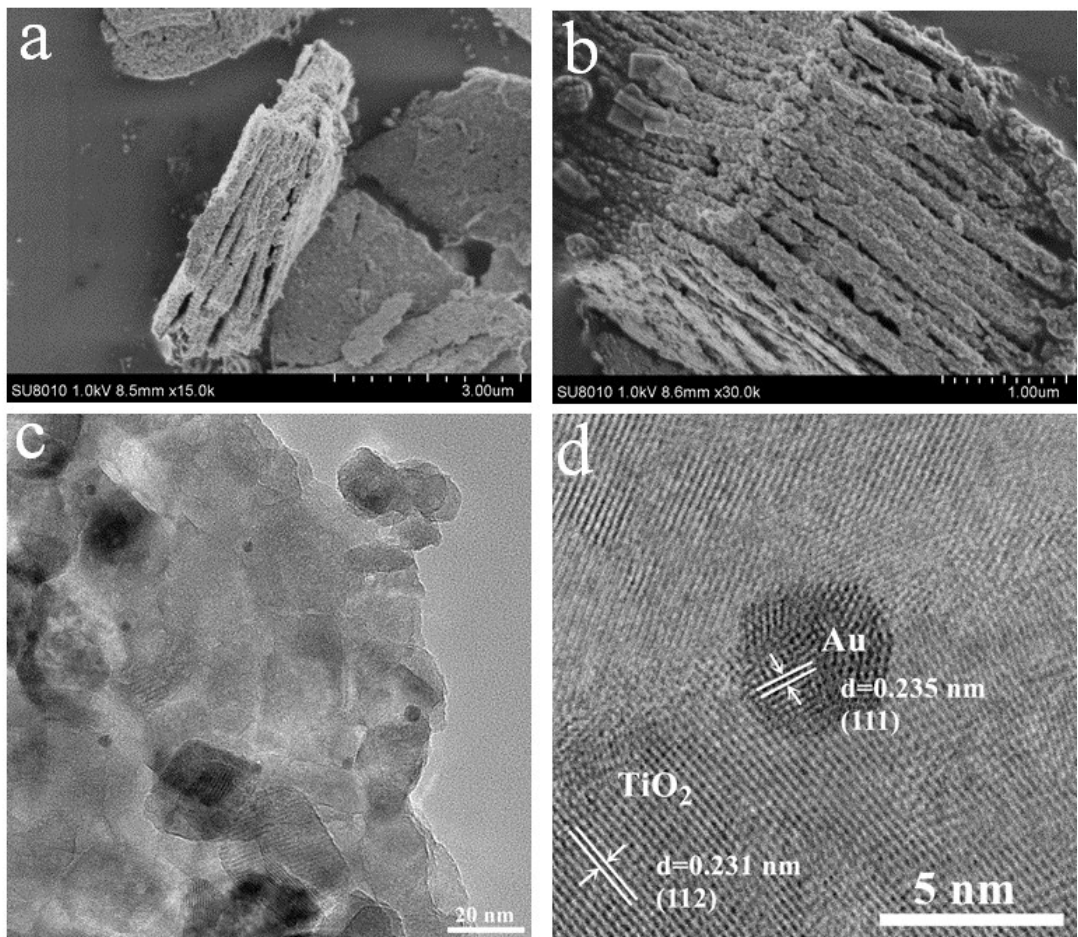


Figure S2: Morphology and structure analysis for pure 1wt% Au/TiO₂ sample, (a-b) SEM images; (c-d) TEM images with different magnifications.

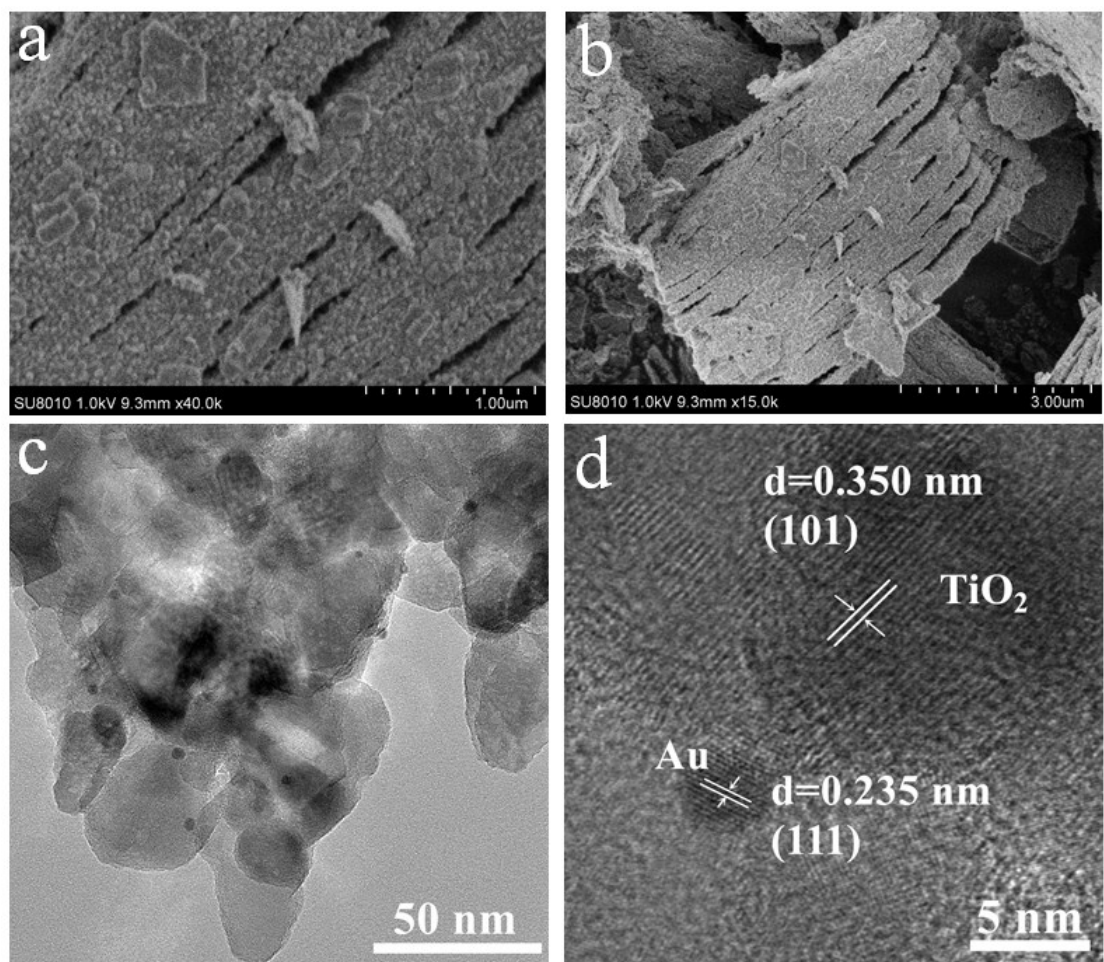


Figure S3: Morphology and structure analysis for 3wt% Au/TiO₂ sample, (a-b) SEM images; (c-d) TEM images with different magnifications.

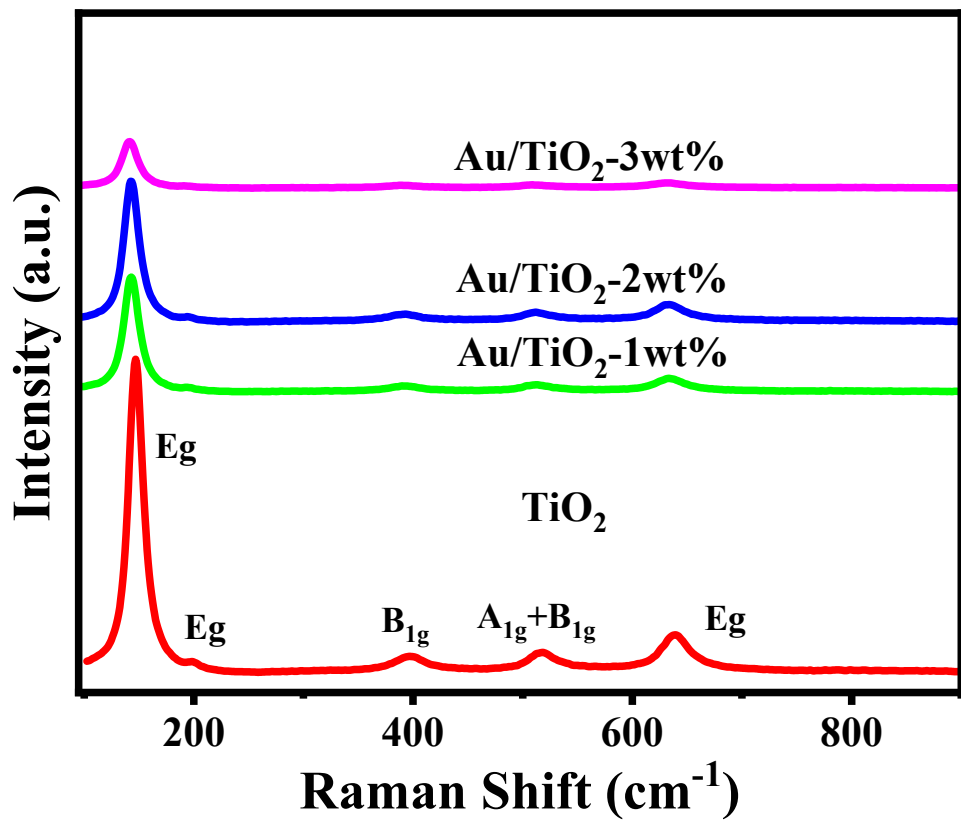


Figure S4: Raman spectra analysis for pure TiO_2 and Au/TiO_2 samples with different gold loading amounts.

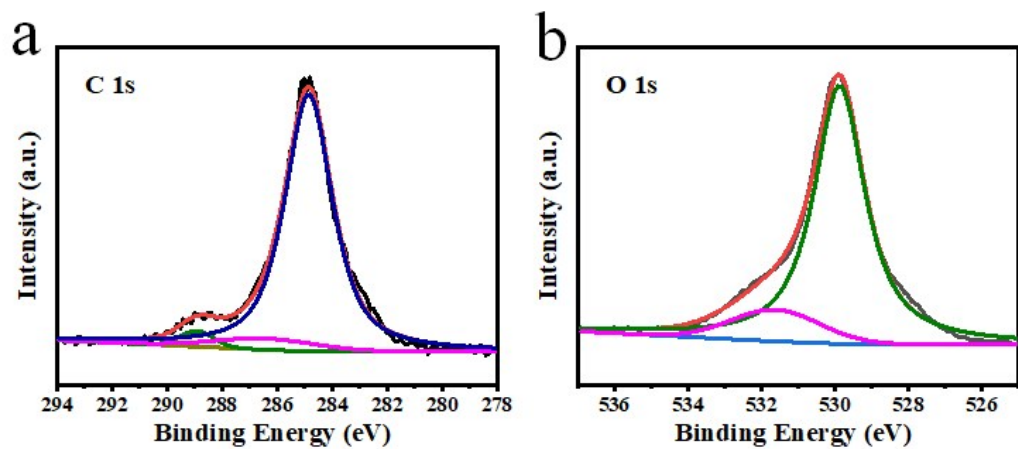


Figure S5: XPS spectrum for pure TiO_2 sample, (a) XPS of C 1s; (b) XPS of O 1s.

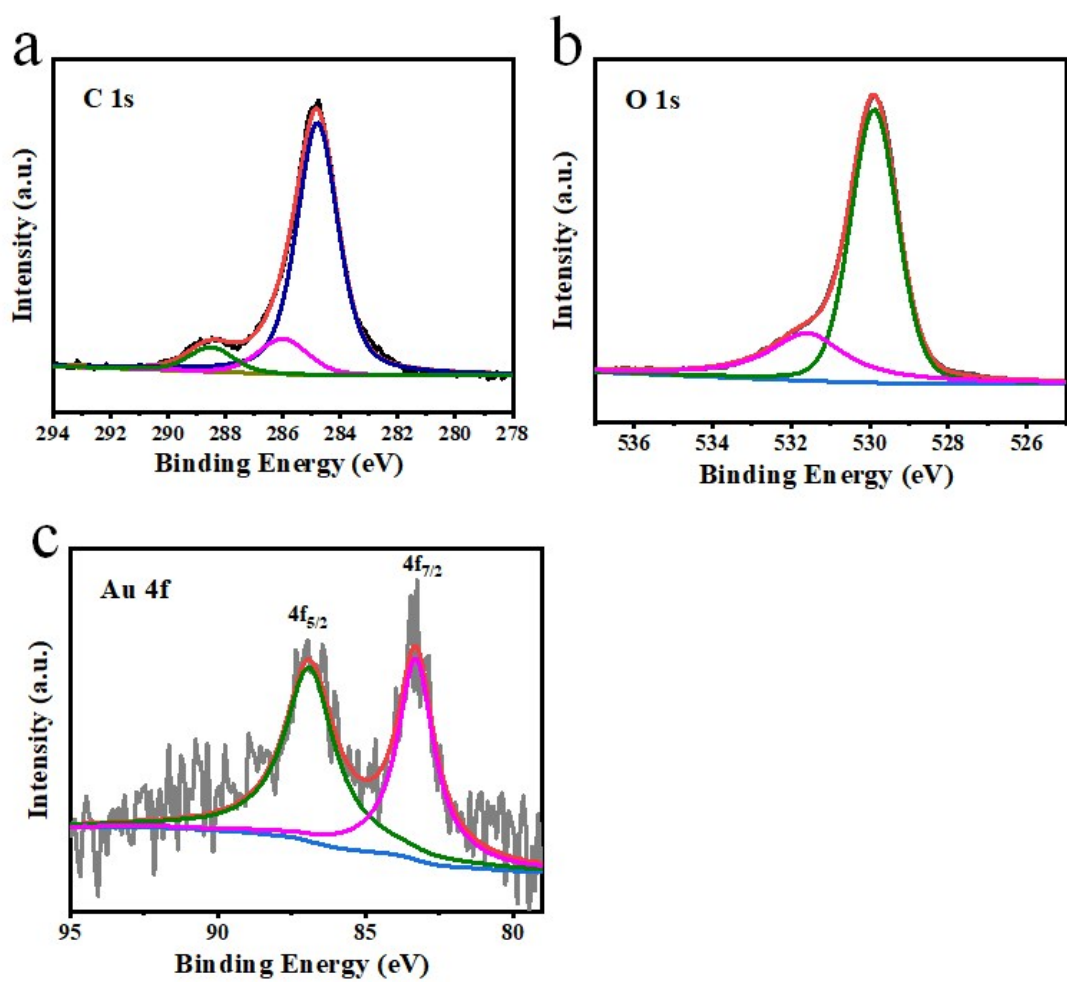


Figure S6: XPS spectrum for the prepared 1 wt% Au/ TiO_2 sample, (a) XPS of C 1s; (b) XPS of O 1s; (c) XPS of Au 4f.

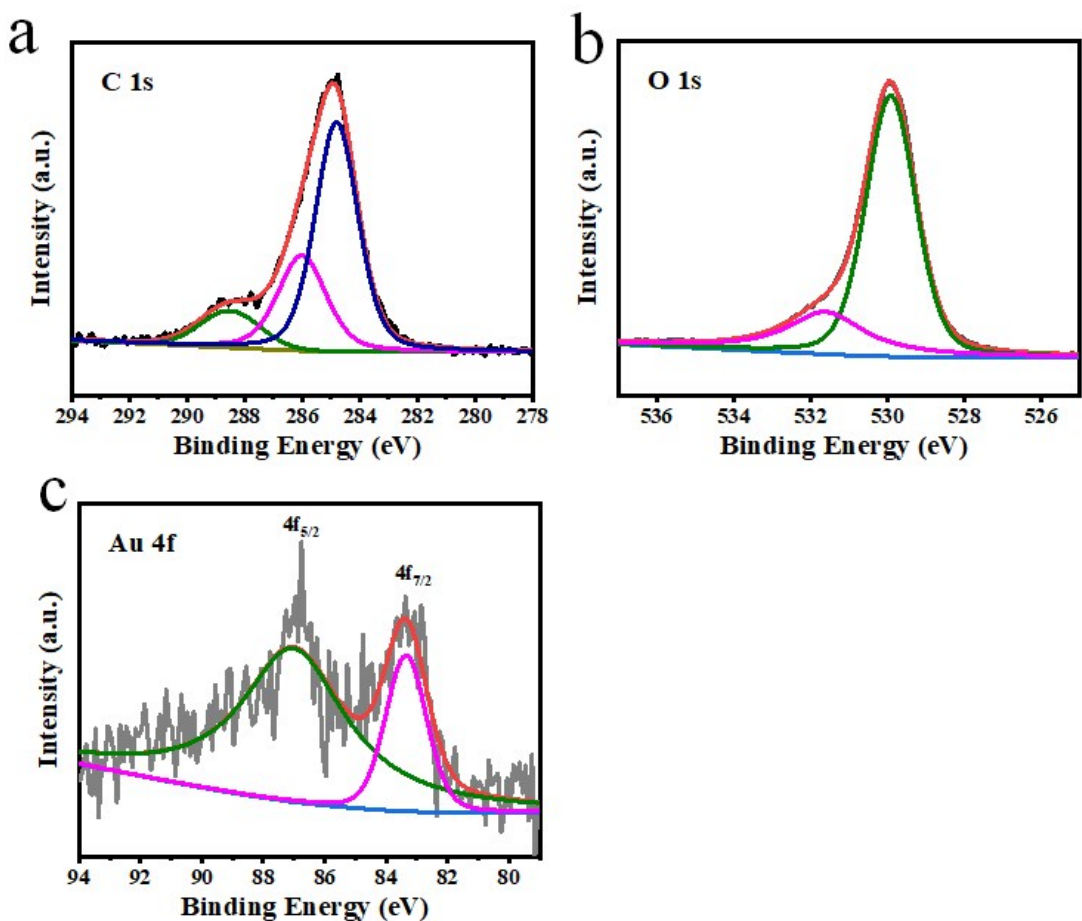


Figure S7: XPS spectrum for the prepared 3wt% Au/TiO₂ sample, (a) XPS of C 1s; (b) XPS of O 1s; (c) XPS of Au 4f.

Table S1: Au L₃-edge EXAFS fitting results (R : distance; CN : coordination number; σ^2 : Debye-Waller factor; ΔE_0 : inner potential correction) of 2wt% Au/TiO₂.

Sample	Au-O		Au-Au		σ^2 (Å ²)	ΔE_0 (eV)
	R (Å)	CN	R (Å)	CN		
2wt% Au/TiO ₂	—	—	2.91±0.02	9.0±0. 9	0.008	7.8±1.8

R : distance; CN : coordination number; σ^2 : Debye-Waller factor; ΔE_0 : inner potential correction

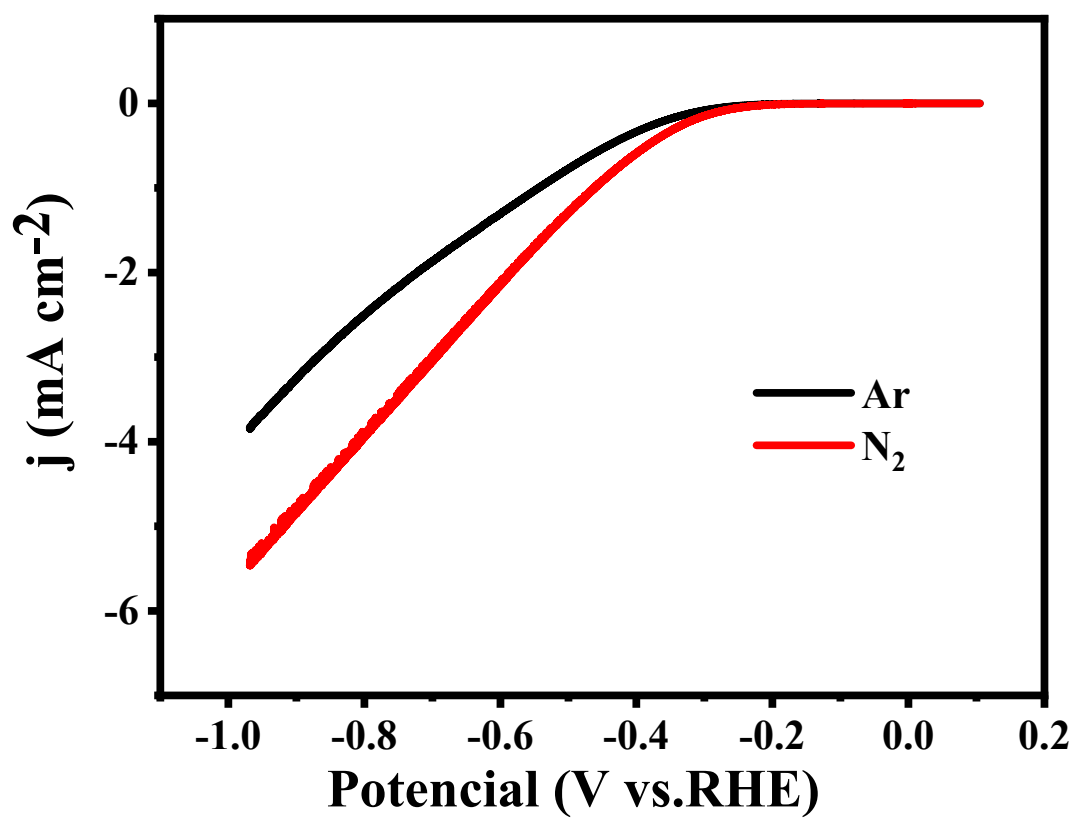


Figure S8: Linear sweep voltammetry (LSV) curves for 2wt% Au/TiO₂ in N₂-saturated and Ar-saturated 0.01 M HCl solution.

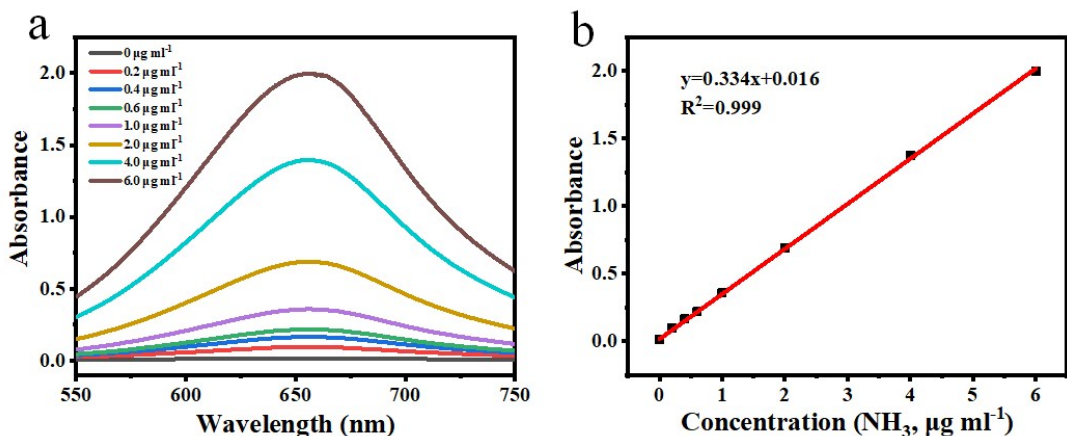


Figure S9: (a) UV-Vis absorption spectra of indophenol assays with NH_4^+ ions after incubated for 2 h at room temperature. (b) Calibration curve used for estimation of NH_3 from the NH_4^+ ion concentration.

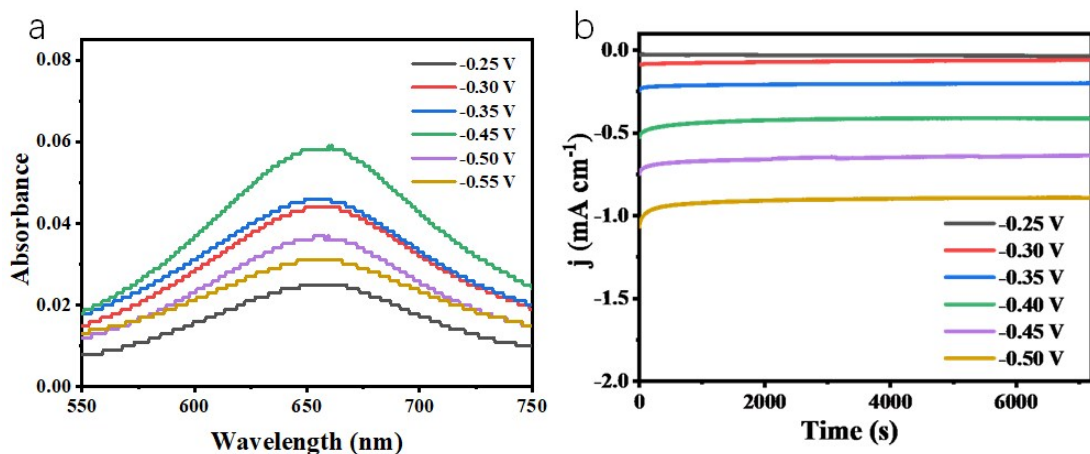


Figure S10: (a)UV-Vis absorption spectra of the 2wt% Au/TiO₂ stained with indophenol indicator after NRR electrolysis for 2 h and (b) Chronoamperometry results of electrode recorded at various potentials

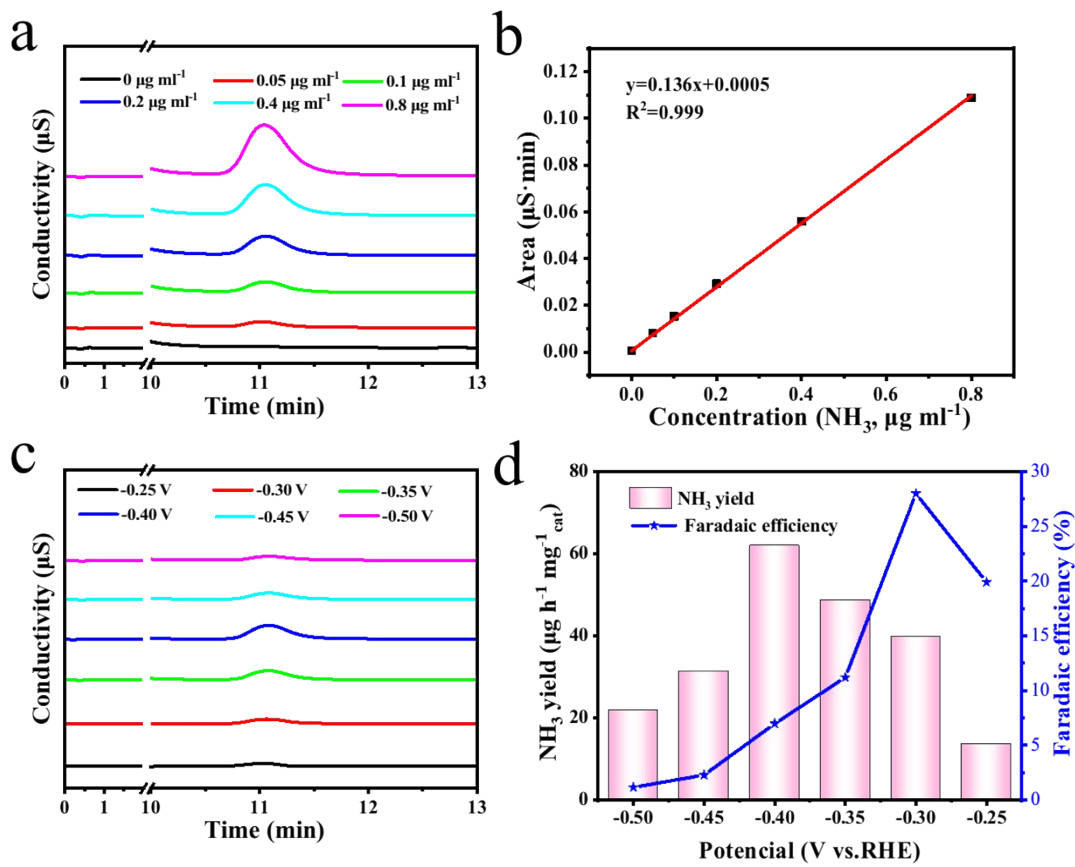


Figure S11: Ion-chromatogram testing for the prepared 2wt% Au/TiO₂ hybrid catalyst, (a) Ion chromatogram curves for the standard NH_4^+ ions. (b) Calibration curve used for estimation of NH_4^+ . (c) Ion chromatogram for the electrolytes at a series of potentials after electrolysis for 2 h. (d) NH_3 yield rate and Faradaic efficiency at corresponding potentials

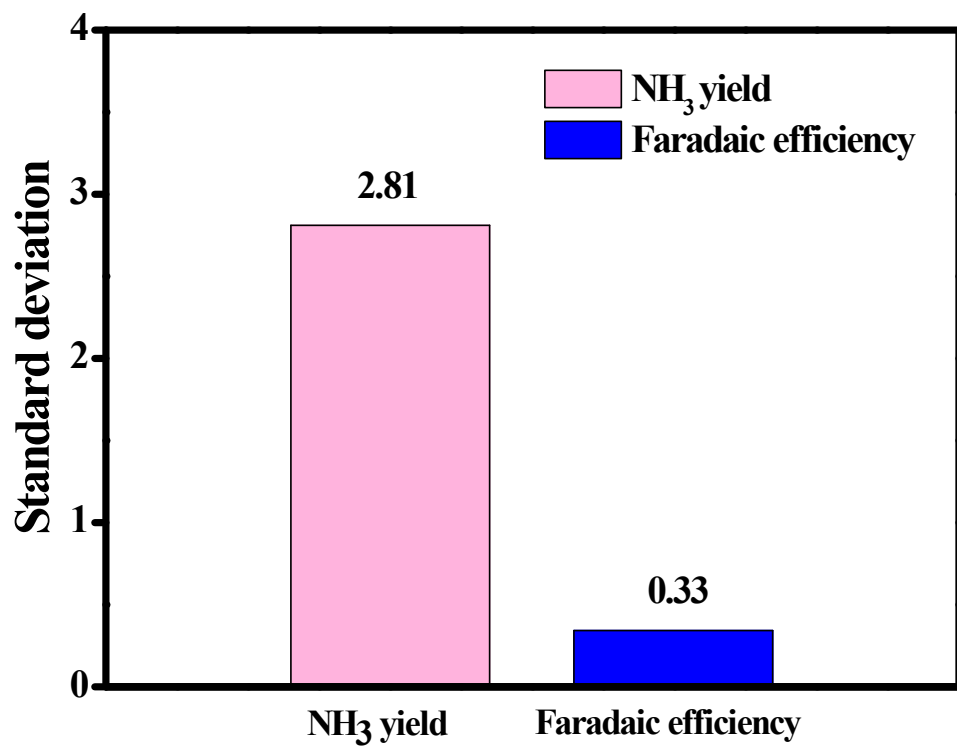


Figure S12: The standard deviation plot for NH₃ yield rate and FE of 2 wt% Au/TiO₂ hybrid after 5 cycles at a potential of -0.4 V under ambient conditions.

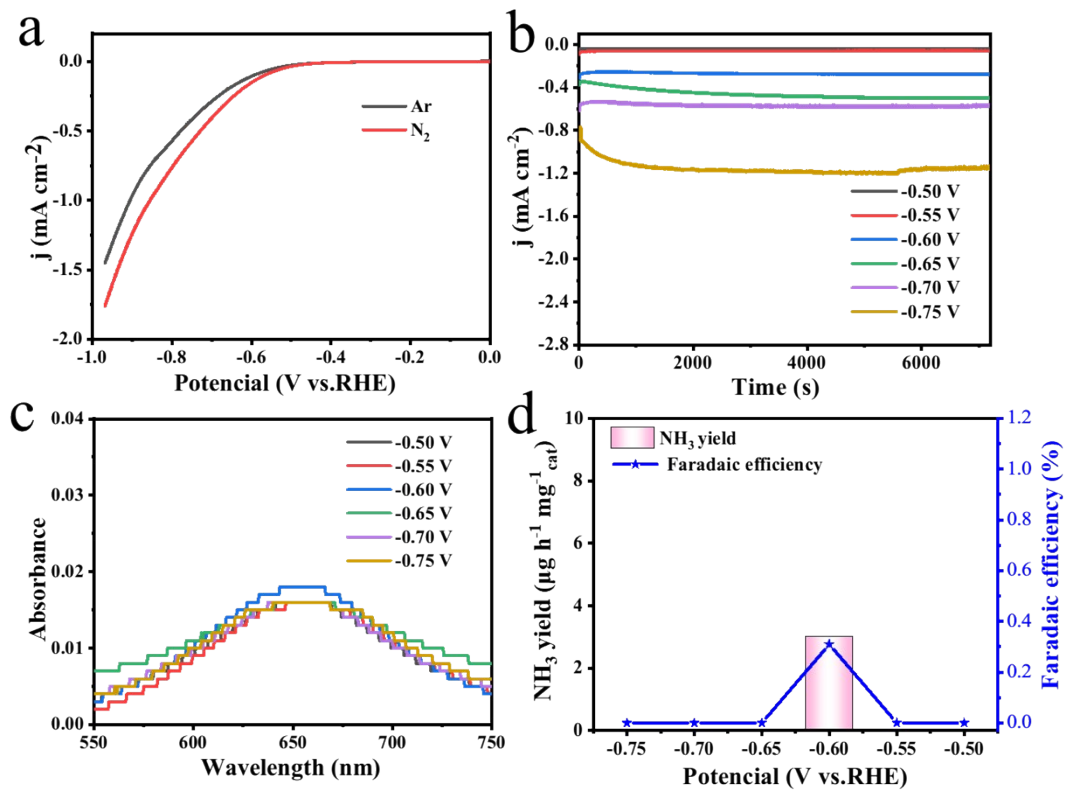


Figure S13: NRR testing for the prepared TiO_2 (a) Linear sweep voltammetry (LSV) curves of electrode recorded in N_2 -saturated and Ar-saturated 0.01 M HCl solution (b) Chronoamperometry results at various potentials (c) Corresponding UV-vis absorption spectra of the electrolyte stained with indicator for NH_3 . (d) Faradaic efficiency and NH_3 yield rate at various potentials

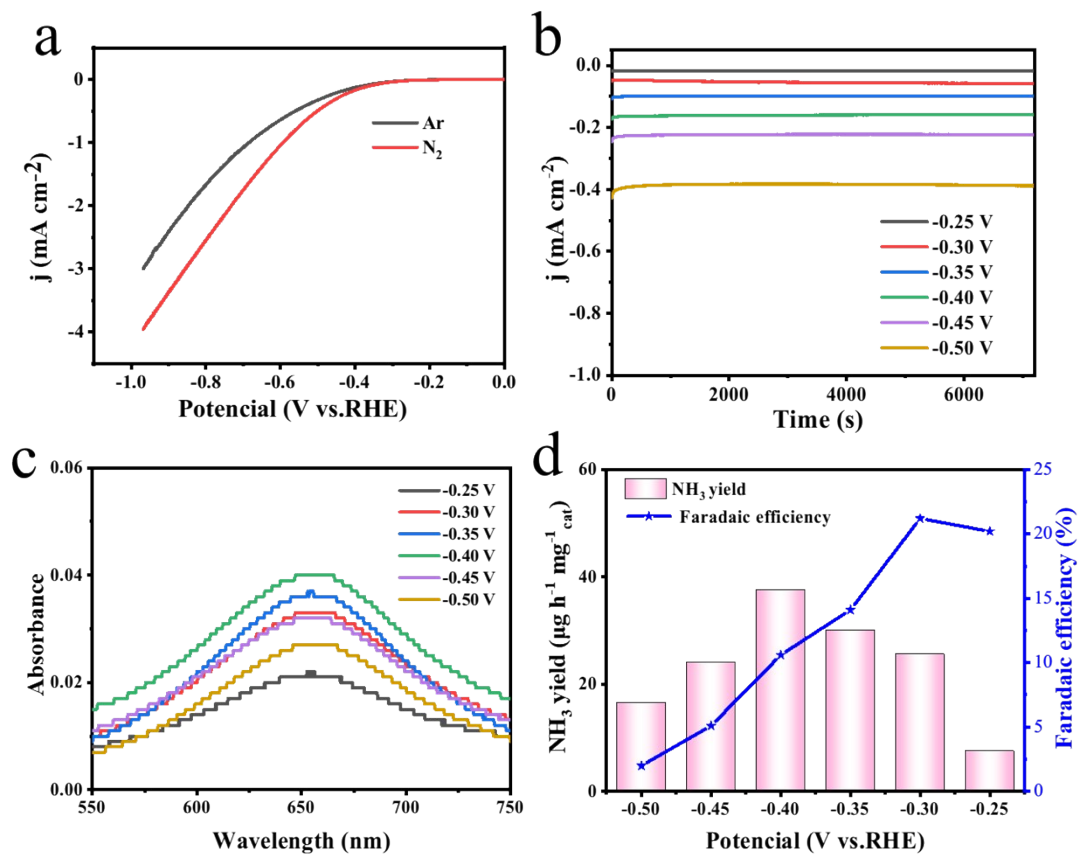


Figure S14: NRR testing for the prepared 1wt% Au/TiO₂ sample, (a); NH₃ yield rate and Faradaic efficiency at each potential. (b) UV-Vis absorption spectra of the electrolytes stained with indophenol indicator after NRR electrolysis for 2h.

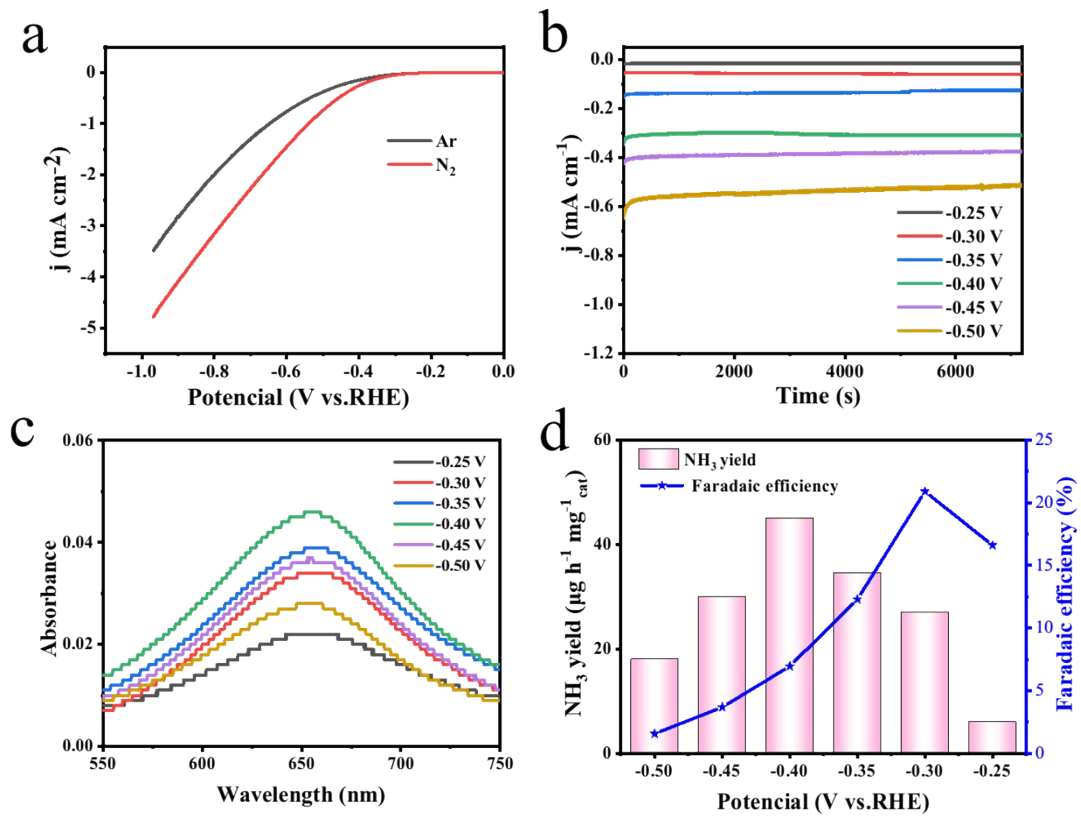


Figure S15: NRR testing for the prepared 3wt% Au/TiO₂ sample, (a) NH₃ yield rate and Faradaic efficiency at each potential. (b) UV-Vis absorption spectra of the electrolytes stained with indophenol indicator after NRR electrolysis for 2h.

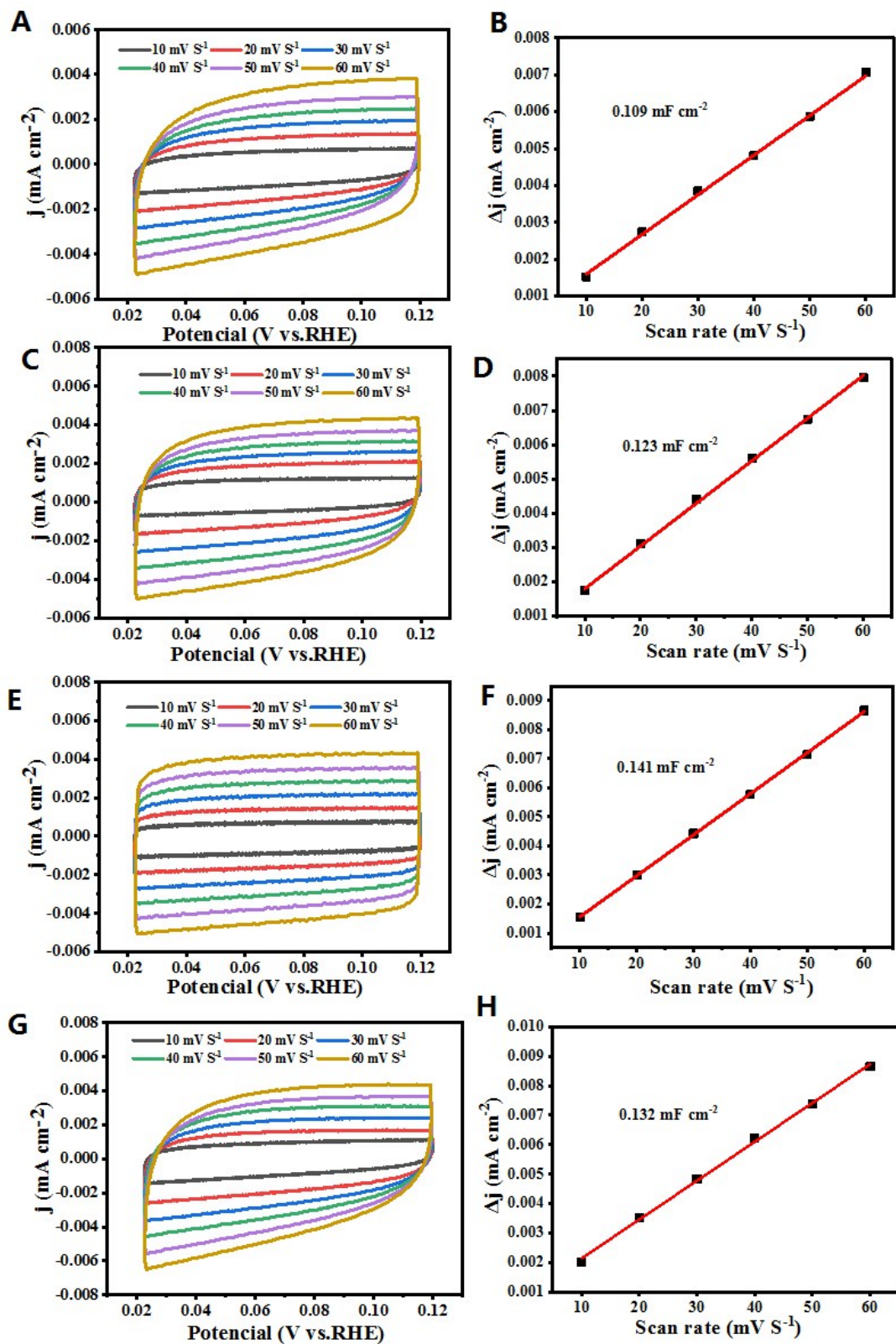


Figure S16: CV and the calculated ECSAs results of the pure TiO_2 and Au/TiO_2 samples with different gold loading amounts, (A-B) TiO_2 ; (C-D) 1wt% Au/TiO_2 ; (E-F) 2wt% Au/TiO_2 ; (G-H) 3wt% Au/TiO_2 .

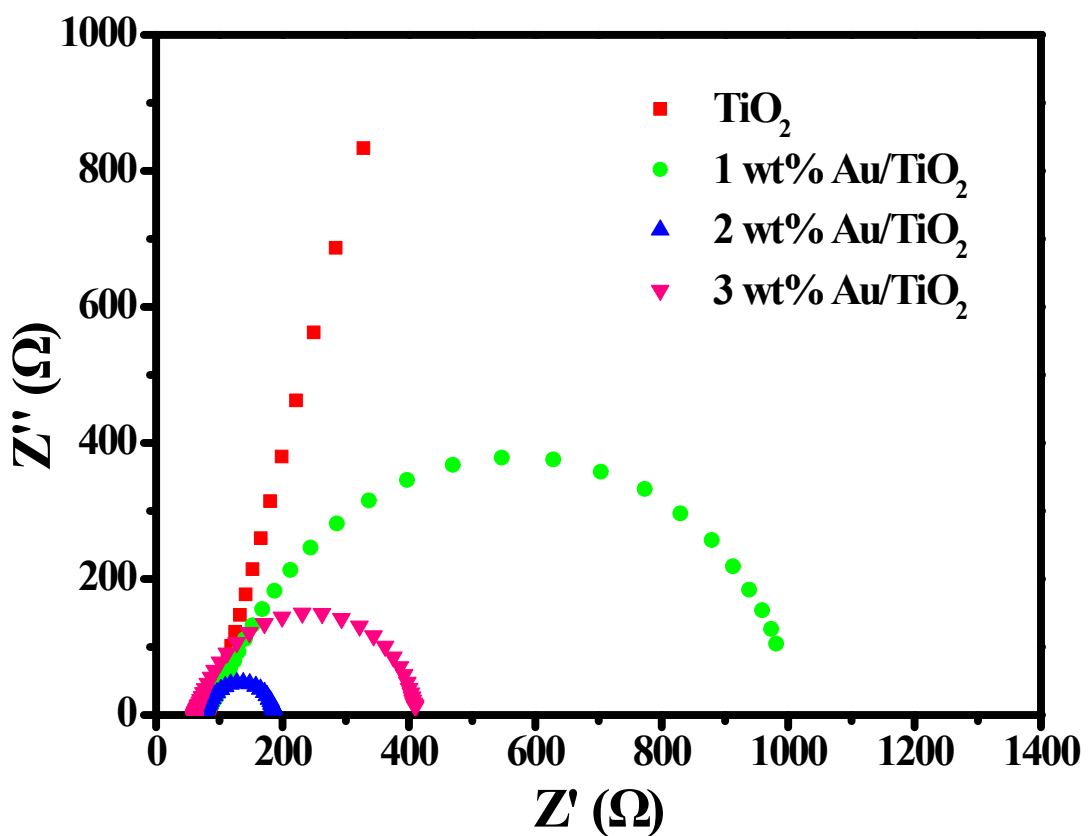


Figure S17: EIS testing for pure TiO_2 and Au/TiO_2 samples with different gold loading amounts.

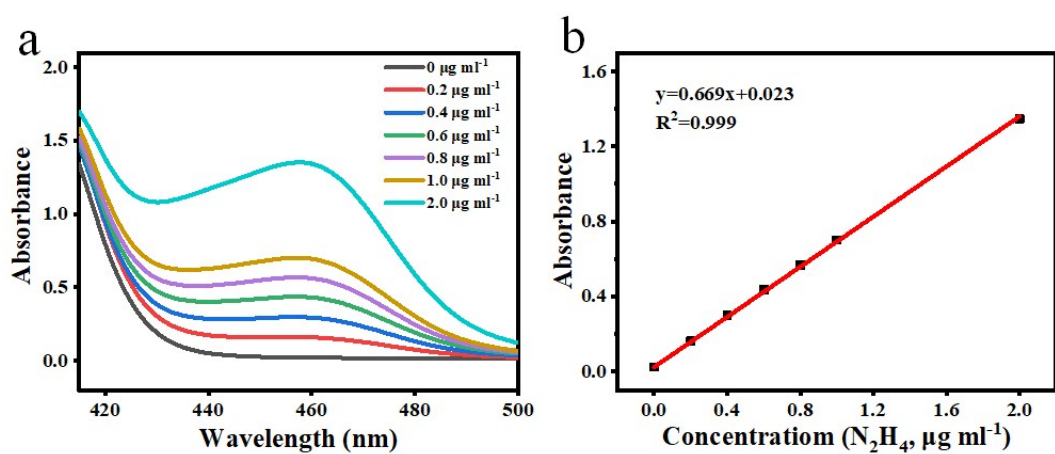


Figure S18: (a) (a) UV-vis curves of various $\text{N}_2\text{H}_4 \cdot \text{H}_2\text{O}$ concentrations after incubation

for 10 min at room temperature. (b) Calibration curve used for estimation of $\text{N}_2\text{H}_4 \cdot \text{H}_2\text{O}$ concentration.

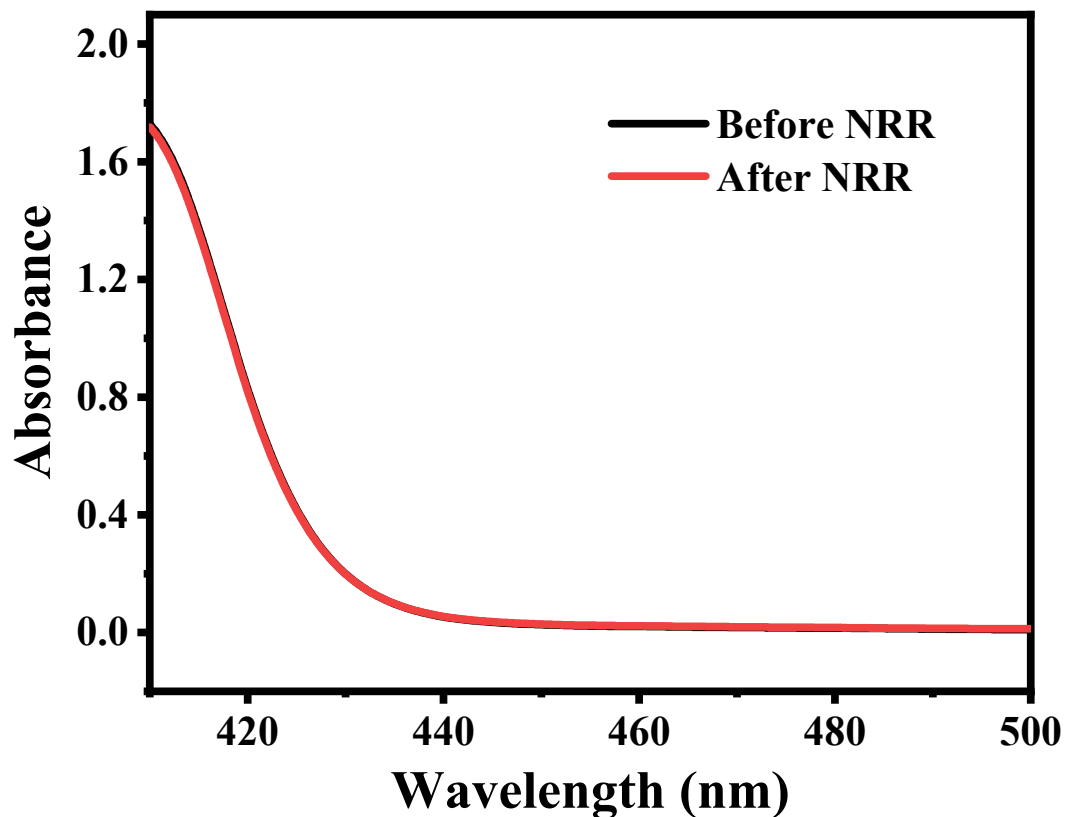


Figure S19: UV-Vis absorption spectra of the electrolytes estimation by the method of Watt and Chrisp before and after 2 h electrolysis in N_2 atmosphere at -0.40 V.

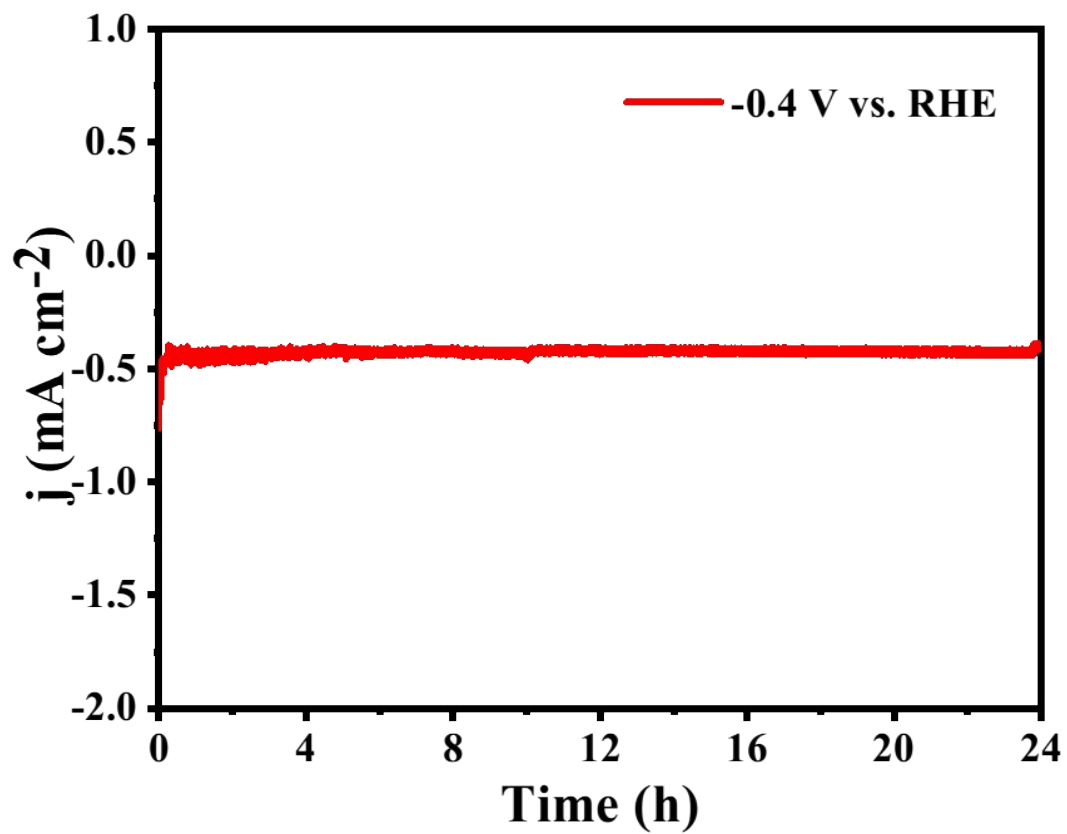


Figure S20: Time-dependent current density curve for the 2wt% Au/TiO₂ catalyst at -0.40 V for 24 h.

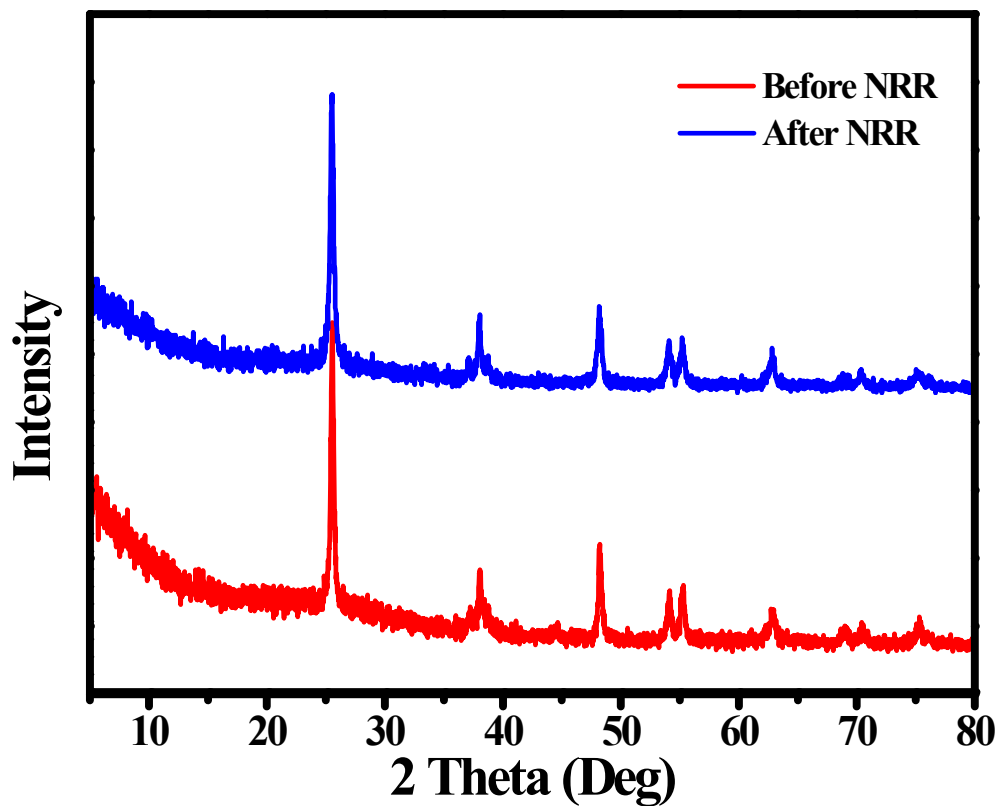


Figure S21: XRD patterns analysis for the prepared 2wt% Au/TiO₂ hybrid catalyst before and after long-term cycling NRR

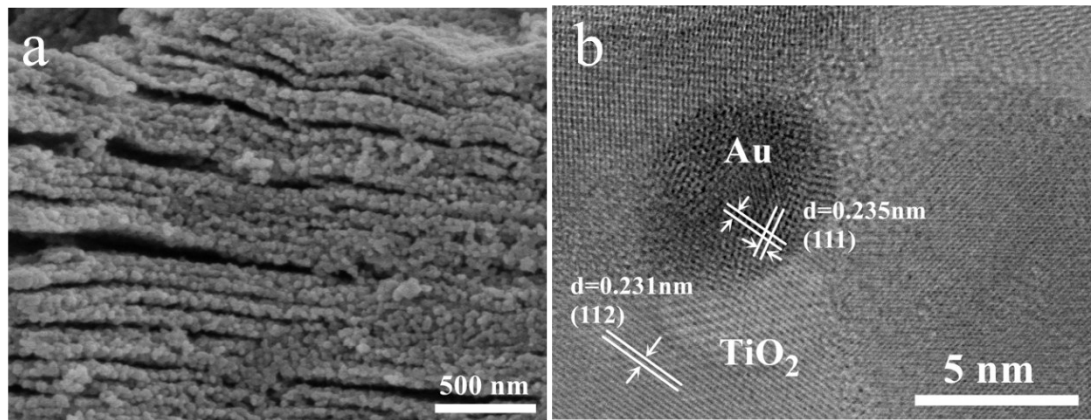


Figure S22: Morphology analysis for the prepared 2wt% Au/TiO₂ hybrid catalyst before and after long-term cycling NRR, (a) SEM image; (b) HRTEM image after long-term NRR catalysis.

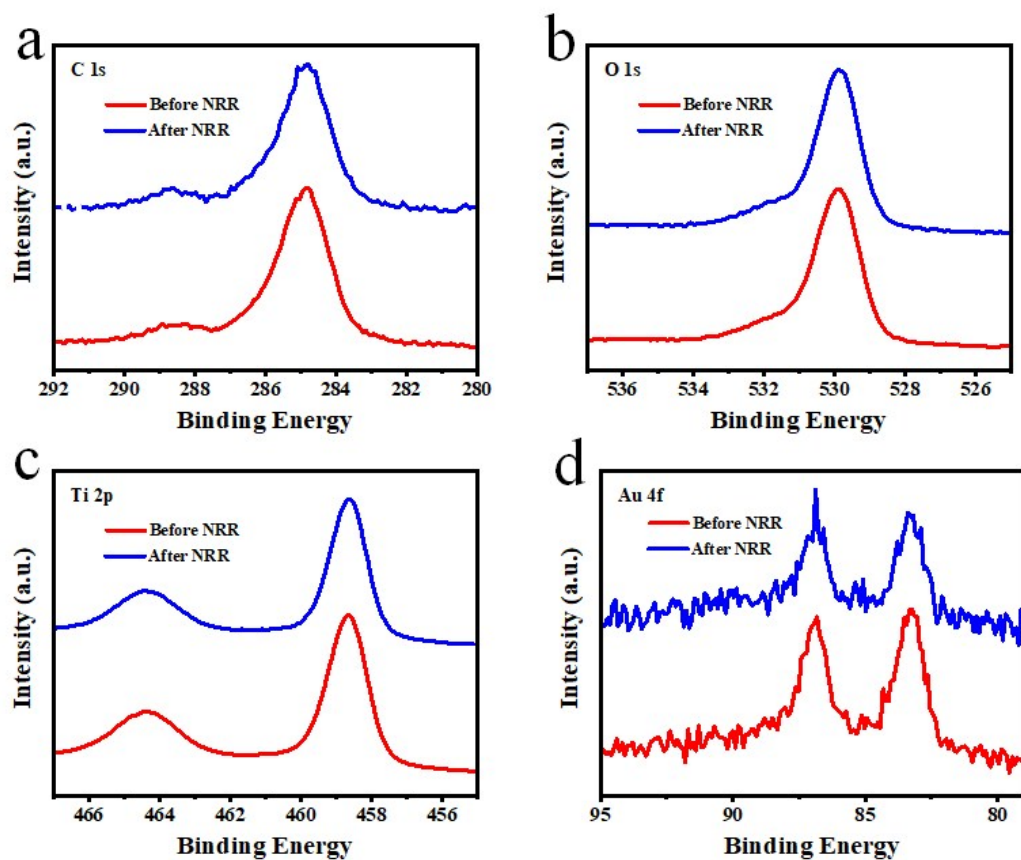


Figure S23: XPS spectrum analysis for the prepared 2wt% Au/TiO₂ hybrid catalyst before and after long-term cycling NRR.

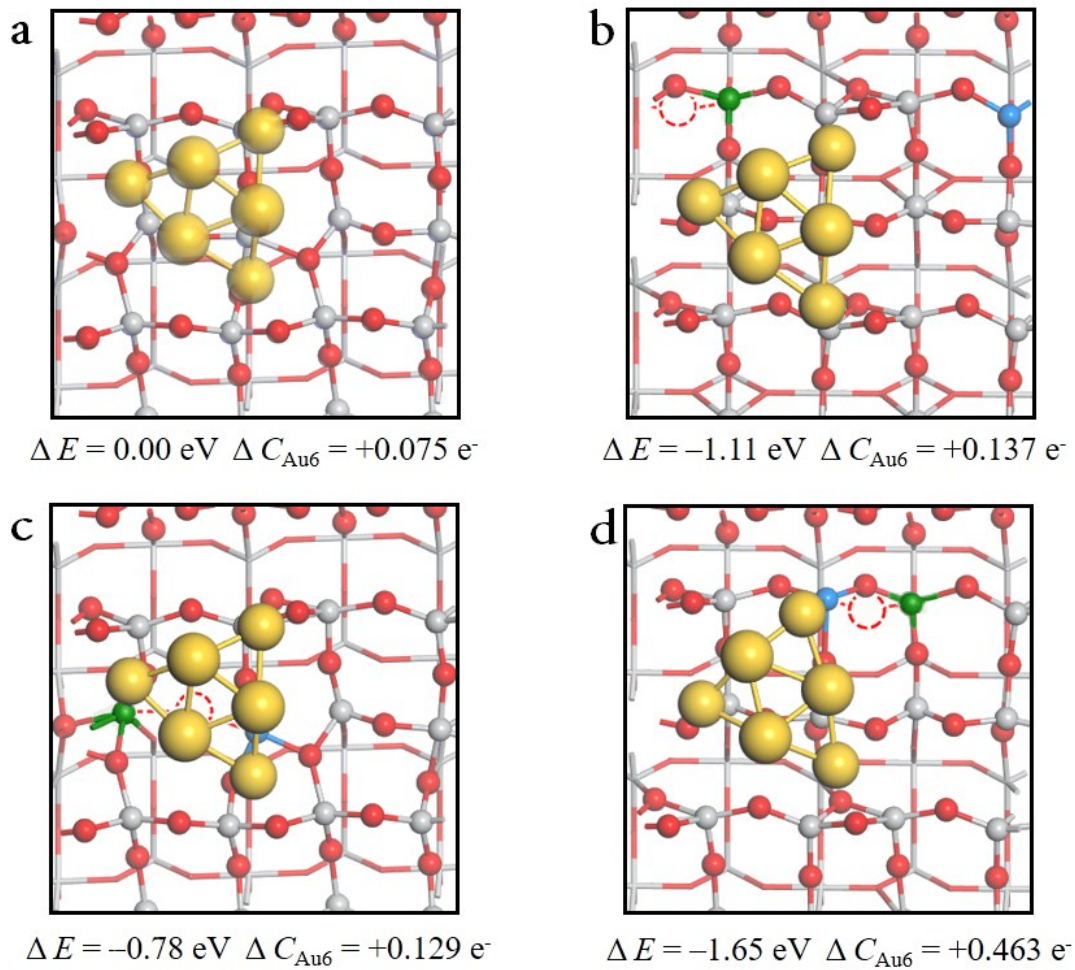


Figure S24. Structure of Au_6 cluster adsorbed on different site of $\text{TiO}_2(112)$ surface. The adsorption energy relative to Au_6 on perfect $\text{TiO}_2(112)$ and the amount of electron transferred from the substrate were given below.

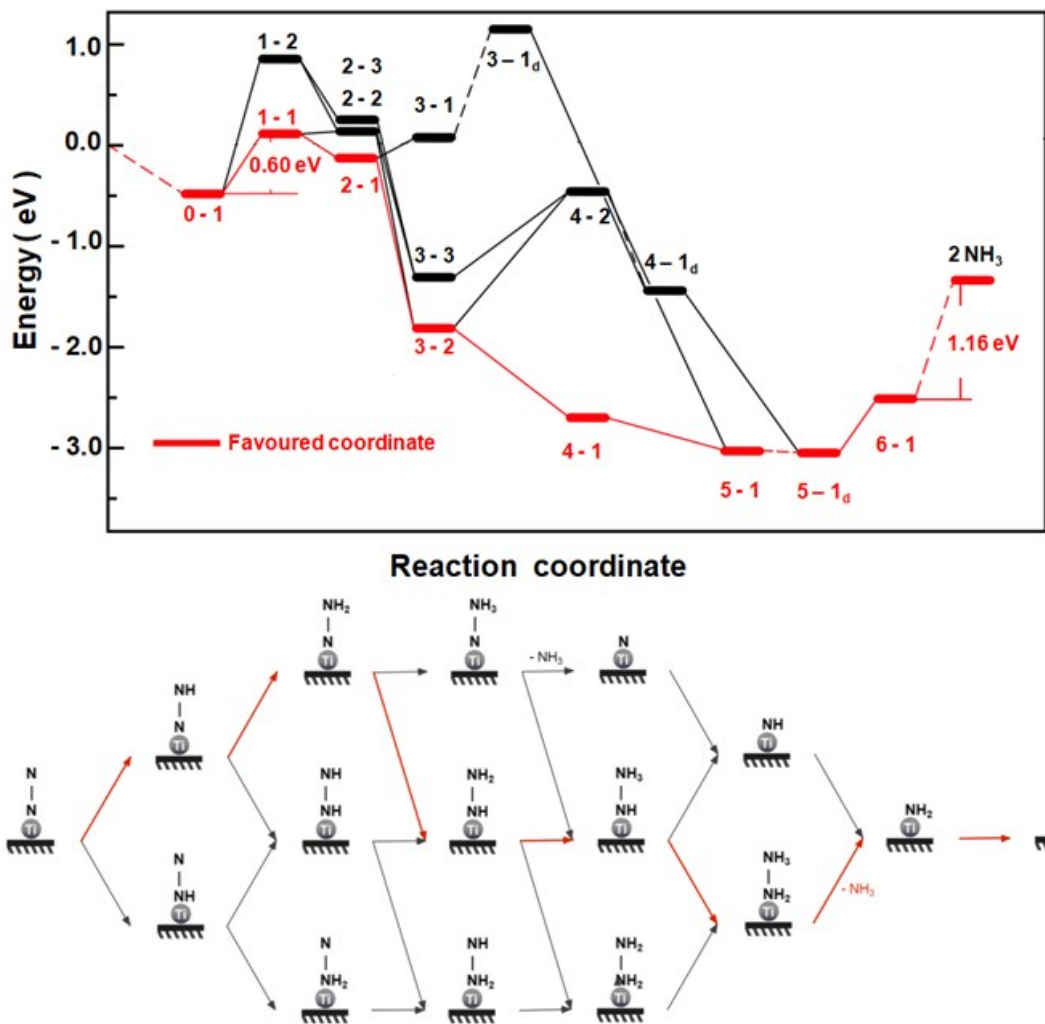


Figure S25. Possible reaction pathways of NRR on TiO₂-V_O surface. Red line shows the most favorable reaction route.

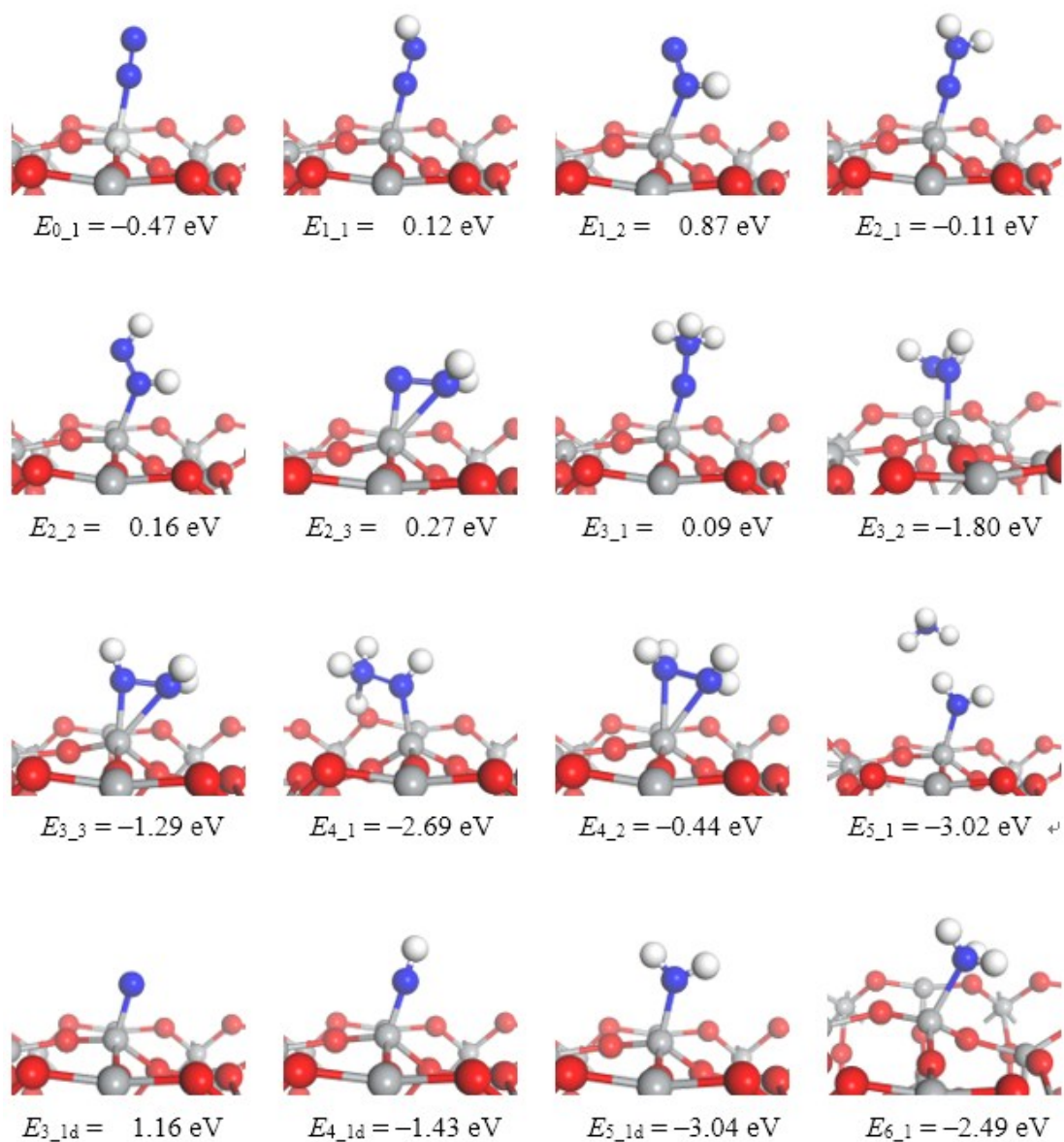


Figure S26. The structure and energy of the species labeled in Figure S25.

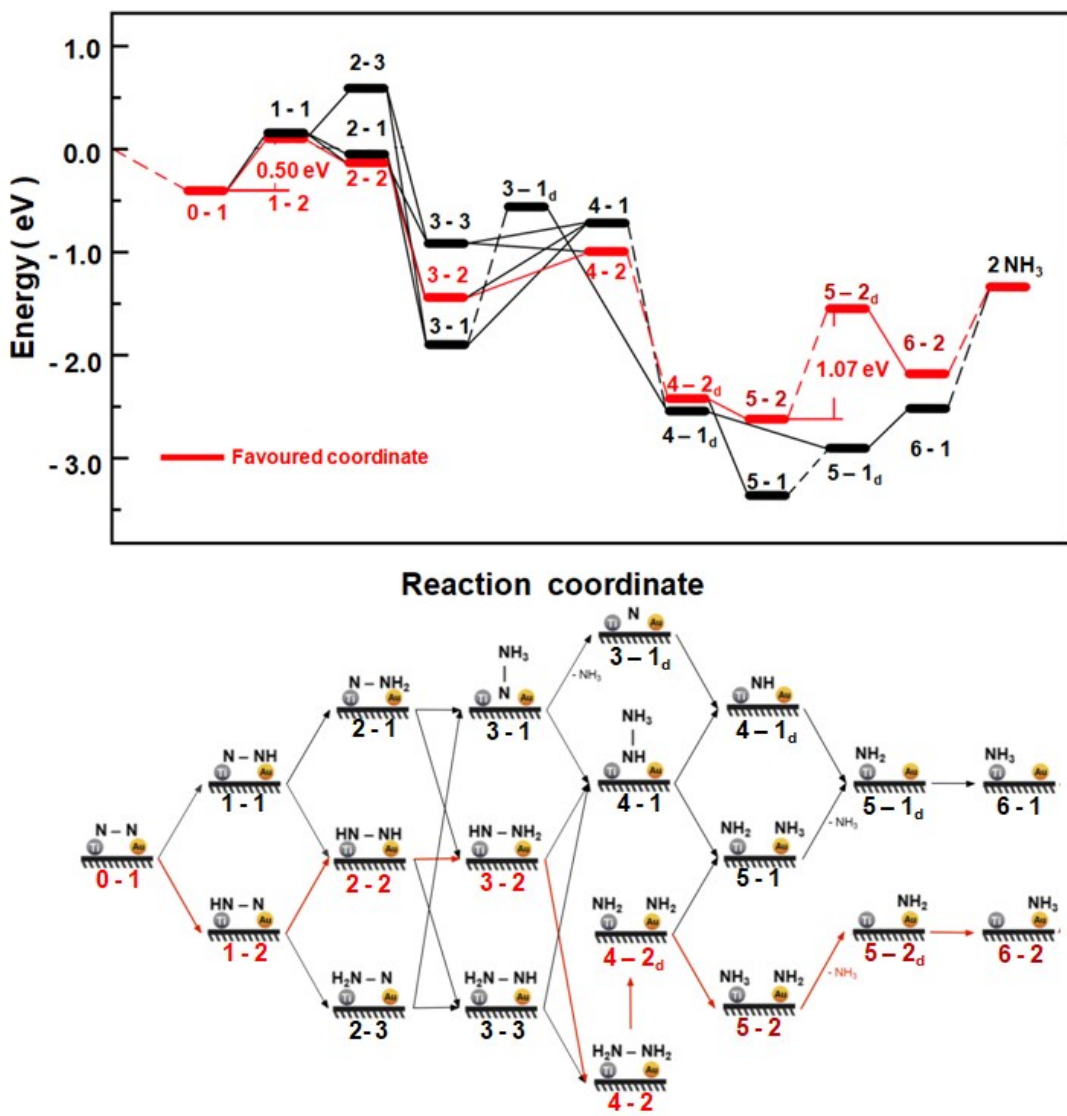


Figure S27. Possible reaction routes of NRR on Au₆/TiO₂-V_O surface. Red line shows the most favorable route.

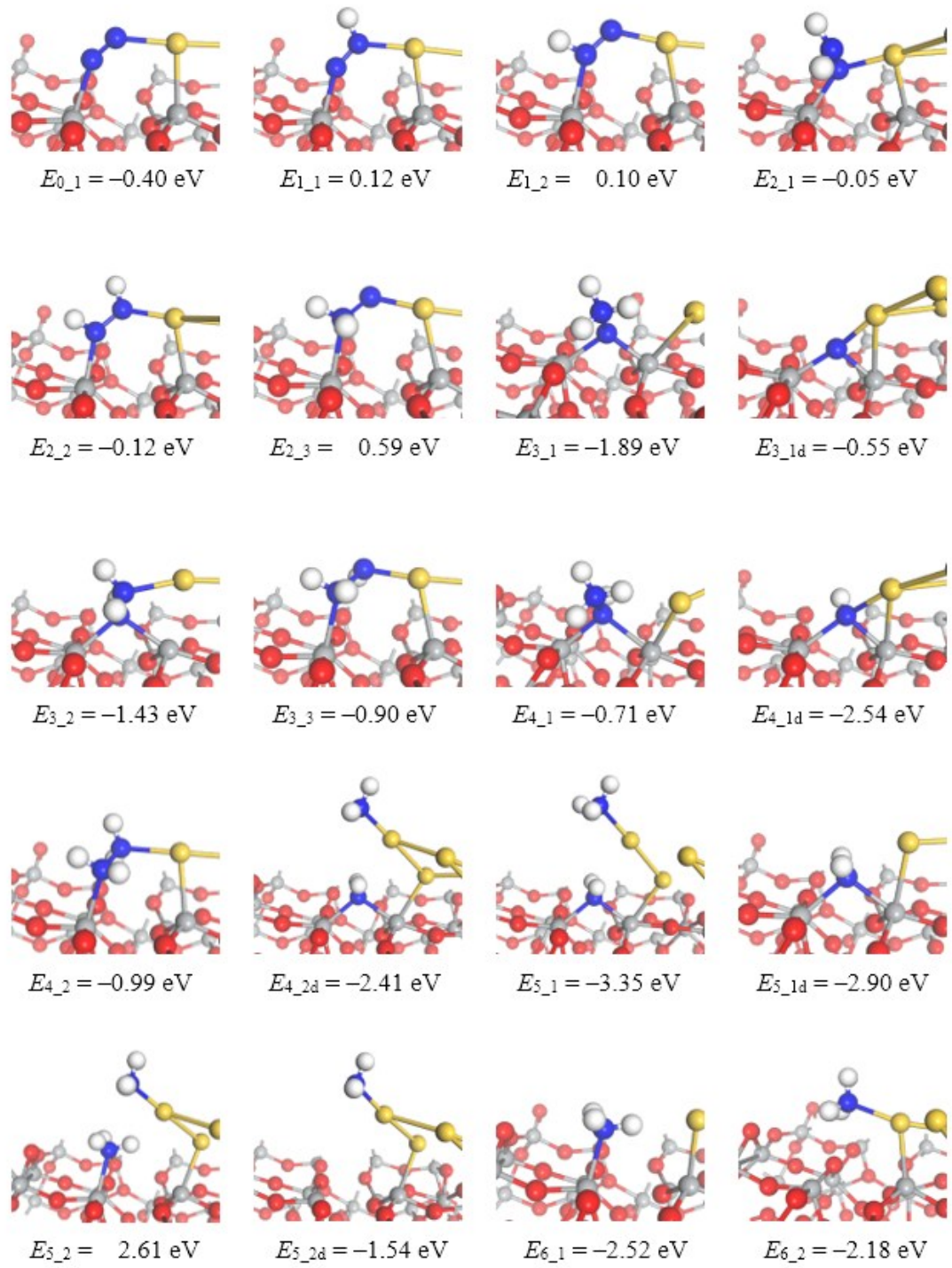


Figure S28. The structure and energy of the species labeled in Figure S27.

Table S2. Adsorption Characteristics of Au₆ Cluster, N₂ and H⁺ on Different Surfaces

	TiO ₂ -V _O	Au ₆ /TiO ₂	Au ₆ /TiO ₂ -V _O
□E _{ads-Au₆} / eV	—	0.00	-1.65
□C _{Au₆} ^a / e ⁻	—	0.075	0.463
□E _{ads-H⁺-max} / eV	-0.59	0.12	-0.59
□E _{ads-N₂-max} / eV	-0.47	-0.14	-0.40
□d _{N-N} ^b / Å	0.026	0.000	0.029

^a Amount of electrons transferred from TiO₂ or TiO₂-V_O to Au₆ cluster. ^b Increase of N-N bond length with respect to that of gas-phase N₂.

Table S3. The adsorption energies of N₂ on different adsorption sites of TiO₂-V_O, Au₆/TiO₂, and Au₆/TiO₂-V_O. The number (n) means the nth stable adsorption site in Figure 1(d – f).

	TiO ₂ - V _O		Au ₆ /TiO ₂		Au ₆ /TiO ₂ - V _O	
	Δ E _{ads} / eV	Δ d _{N-N} / Å	Δ E _{ads} / eV	Δ d _{N-N} / Å	Δ E _{ads} / eV	Δ d _{N-N} / Å
Site 1	-0.47	0.026	-0.14	0.000	-0.40	0.029
Site 2	-0.22	0.000	-0.06	0.001	-0.21	0.002
Site 3	-0.04	0.001	-0.05	0.001	-0.05	0.001

Table S4. The adsorption energies of H⁺ on different adsorption sites of TiO₂-V_O, Au₆/TiO₂, and Au₆/TiO₂-V_O. The number (n) means the nth stable adsorption site in Figure 1(g – i).

	TiO ₂ -V _O	Au ₆ /TiO ₂	Au ₆ /TiO ₂ -V _O
Site 1	–0.59 eV	0.12 eV	– 0.59 ev
Site 2	0.07 eV	0.84 eV	– 0.36 ev
Site 3	0.00 eV	0.71 eV	– 0.53 ev
Site 4	0.13 eV	0.17 eV	– 0.17 ev
Site 5	—	—	– 0.11 eV

Table S5. The d band center, valence band center and conduction band center of Ti and Au atoms participated in the adsorption of N₂.

band center	<i>d</i> _{total}	<i>d</i> _{xy}	<i>d</i> _{xz}	<i>d</i> _{yz}	<i>d</i> _{x²-y²}	<i>d</i> _{z²}	
TiO ₂ -V _O	Ti _a -d	–1.41	–1.75	–0.71	–1.51	–2.62	–0.81
	Ti _a -V	–5.54	–6.35	–5.04	–4.56	–7.83	–3.46
	Ti _a -C	0.71	1.12	0.40	0.73	1.07	0.64
Au ₆ /TiO ₂ -V _O	Au _ d	–4.01	–3.81	–4.1	–3.98	–3.89	–4.38
	Au _ V	–4.25	–4.00	–4.38	–4.23	–4.06	–4.69
	Au _ C	1.65	2.12	1.73	1.52	1.64	1.36
Au ₆ /TiO ₂	Ti _b -d	–0.38	–0.38	–0.11	–0.16	–0.44	–1.53
	Ti _b -V	–4.81	–4.81	–5.11	–2.67	–6.72	–6.27
	Ti _b -C	1.83	1.82	1.43	1.53	2.69	1.98

Table S6: NRR Comparison of our catalysts with previously reported electrocatalysts

Catalyst	Electrolyte	NH ₃ yield μg h ⁻¹ mg ⁻¹ _{cat}	FE (%)	Ref.
2 wt% Au/TiO ₂	0.01 M HCl	64.6	29.5	This work
TiO ₂	0.1 M Na ₂ SO ₄	5.6	2.5	1
TiO ₂ -rGO	0.1 M Na ₂ SO ₄	15.13	3.3	2
V-TiO ₂	0.5 M LiClO ₄	17.76	15.3	3
C-doped TiO ₂	0.5M Na ₂ SO ₄	16.22	1.84	4
Au-Fe ₃ O ₄	0.1 M HCl	21.42	10.54	5
B-doped TiO ₂	0.1 M Na ₂ SO ₄	14.4	3.4	6
TiO ₂ /Ti ₃ C ₂ T _x	0.1 M HCl	32.17	16.07	7
Au/Ti ₃ C ₂	0.1 M HCl	30.06	18.34	8
Au nanorods	0.1 M KOH	1.648	4.02	9
AuSAs-NDPCs	0.1M HCl	2.32	12.3	10
Au HNCs	0.5 M LiClO ₄	3.96	35.9	11
a-Au/CeOx-RGO	0.1 M HCl	8.3	10.1	12
Au Nanoclusters on TiO ₂	0.1 M HCl	21.4	8.11	13
Au/CeO ₂	0.01 M H ₂ SO ₄	28.2	9.5	14
Au/Ni	0.1 M Na ₂ SO ₄	9.42	13.36	15
Au flower	0.1 M HCl	35.57	6.05	16

Ru SAs/N-C	0.05 M H ₂ SO ₄	120.9	29.6	17
Ru NPs	0.01 M HCl	21.4	5.4	18
Defect-rich MoS ₂	0.1 M Na ₂ SO ₄	29.28	8.34	19
Au/NCM	0.1 M HCl	36	22	20
Au ₁ /C ₃ N ₄	5 mM H ₂ SO ₄	1.96	11.1	21
Au nanocage	0.5 M LiClO ₄	2.35	30.2	22

References:

1. Zhang, R.; Ren, X.; Shi, X.; Xie, F.; Zheng, B.; Guo, X.; Sun, X., Enabling Effective Electrocatalytic N₂ Conversion to NH₃ by the TiO₂ Nanosheets Array under Ambient Conditions. *ACS Appl. Mater. Interfaces.* **2018**, 10, 28251-28255.
2. Zhang, X.; Liu, Q.; Shi, X.; Asiri, A. M.; Luo, Y.; Sun, X.; Li, T., TiO₂ nanoparticles-reduced graphene oxide hybrid: an efficient and durable electrocatalyst toward artificial N₂ fixation to NH₃ under ambient conditions. *J. Mater. Chem. A.* **2018**, 6, 17303-17306.
1. Zhang, R.; Ren, X.; Shi, X.; Xie, F.; Zheng, B.; Guo, X.; Sun, X., Enabling Effective Electrocatalytic N₂ Conversion to NH₃ by the TiO₂ Nanosheets Array under Ambient Conditions. *ACS Appl. Mater. Interfaces.* **2018**, 10, 28251-28255.
2. Zhang, X.; Liu, Q.; Shi, X.; Asiri, A. M.; Luo, Y.; Sun, X.; Li, T., TiO₂ nanoparticles-reduced graphene oxide hybrid: an efficient and durable electrocatalyst toward artificial N₂ fixation to NH₃ under ambient conditions. *J. Mater. Chem. A.* **2018**, 6, 17303-17306.
3. Wu, T.; Kong, W.; Zhang, Y.; Xing, Z.; Zhao, J.; Wang, T.; Shi, X.; Luo, Y.; Sun, X., Greatly Enhanced Electrocatalytic N₂ Reduction on TiO₂ via V Doping. *Small Methods.* **2019**, 1900356.
4. Jia, K.; Wang, Y.; Pan, Q.; Zhong, B.; Luo, Y.; Cui, G.; Guo, X.; Sun, X., Enabling the electrocatalytic fixation of N₂ to NH₃ by C-doped TiO₂ nanoparticles under ambient conditions. *Nanoscale Adv.* **2019**, 1, 961-964.
5. Zhang, J.; Ji, Y.; Wang, P.; Huang, X.; Adsorbing and Activating N-2 on Heterogeneous Au-Fe₃O₄ Nanoparticles for N-2 Fixation, *Adv. Funct. Mater.* **2019**, 1906576.
6. Wang, Y.; Jia, K.; Pan, Q.; Xu, Y.; Liu, Q.; Cui, G.; Guo, X.; Sun, X., Boron-Doped TiO₂ for Efficient Electrocatalytic N₂ Fixation to NH₃ at Ambient Conditions. *ACS Sustainable Chem. Eng.* **2018**, 7, 117-122.
7. Fang, Y.; Liu, Z.; Han, J.; Jin, Z.; Han, Y.; Wang, F.; Niu, Y.; Wu, Y.; Xu, Y., High-Performance Electrocatalytic Conversion of N₂ to NH₃ Using

- Oxygen-Vacancy-Rich TiO₂ In Situ Grown on Ti₃C₂T_x MXene. *Adv. Energy Mater.* **2019**, *9*, 1803406.
- 8. Liu, D.; Zhang, G.; Ji, Q.; Zhang, Y.; Li, J., Synergistic Electrocatalytic Nitrogen Reduction Enabled by Confinement of Nanosized Au Particles onto a Two-Dimensional Ti₃C₂ Substrate. *ACS Appl. Mater. Interfaces*. **2019**, *11*, 25758-25765.
 - 9. Bao, D.; Zhang, Q.; Meng, F. L.; Zhong, H. X.; Shi, M. M.; Zhang, Y.; Yan, J. M.; Jiang, Q.; Zhang, X. B., Electrochemical Reduction of N₂ under Ambient Conditions for Artificial N₂ Fixation and Renewable Energy Storage Using N₂/NH₃ Cycle. *Adv. Mater.* **2017**, *29*, 1604799.
 - 10. Qin, Q.; Heil, T.; Antonietti, M.; Oschatz, M., Single-Site Gold Catalysts on Hierarchical N-Doped Porous Noble Carbon for Enhanced Electrochemical Reduction of Nitrogen. *Small Methods*. **2018**, *2*, 1800202.
 - 11. Nazemi, M.; El-Sayed, M. A., Electrochemical Synthesis of Ammonia from N₂ and H₂O under Ambient Conditions Using Pore-Size-Controlled Hollow Gold Nanocatalysts with Tunable Plasmonic Properties. *J. Phys. Chem. Lett.* **2018**, *9*, 5160-5166.
 - 12. Li, S. J.; Bao, D.; Shi, M. M.; Wulan, B. R.; Yan, J. M.; Jiang, Q., Amorphizing of Au Nanoparticles by CeO_x-RGO Hybrid Support towards Highly Efficient Electrocatalyst for N₂ Reduction under Ambient Conditions. *Adv. Mater.* **2017**, *29*, 1700001.
 - 13. Shi, M. M.; Bao, D.; Wulan, B. R.; Li, Y. H.; Zhang, Y. F.; Yan, J. M.; Jiang, Q., Au Sub-Nanoclusters on TiO₂ toward Highly Efficient and Selective Electrocatalyst for N₂ Conversion to NH₃ at Ambient Conditions. *Adv. Mater.* **2017**, *29*, 1606550.
 - 14. Liu, G.; Cui, Z.; Han, M.; Zhang, S.; Zhao, C.; Chen, C.; Wang, G.; Zhang, H., Ambient Electrosynthesis of Ammonia on a Core-Shell-Structured Au@CeO₂ Catalyst: Contribution of Oxygen Vacancies in CeO₂. *Chem. Eur. J.* **2019**, *25*, 5904-5911.
 - 15. Wang, H.; Yu, H.; Wang, Z.; Li, Y.; Xu, Y.; Li, X.; Xue, H.; Wang, L., Electrochemical Fabrication of Porous Au Film on Ni Foam for Nitrogen Reduction to Ammonia. *Small*. **2019**, *15*, 1804769.
 - 16. Wang, Z.; Li, Y.; Yu, H.; Xu, Y.; Xue, H.; Li, X.; Wang, H.; Wang, L., Ambient Electrochemical Synthesis of Ammonia from Nitrogen and Water Catalyzed by Flower-Like Gold Microstructures. *ChemSusChem*. **2018**, *11*, 3480-3485.
 - 17. Geng, Z.; Liu, Y.; Kong, X.; Li, P.; Li, K.; Liu, Z.; Du, J.; Shu, M.; Si, R.; Zeng, J., Achieving a Record-High Yield Rate of 120.9 μg_{NH₃} mg⁻¹_{cat} h⁻¹ for N₂ Electrochemical Reduction over Ru Single-Atom Catalysts. *Adv. Mater.* **2018**, *1803498*.
 - 18. Wang, D.; Azofra, L. M.; Harb, M.; Cavallo, L.; Zhang, X.; Suryanto, B. H. R.; MacFarlane, D. R., Energy-Efficient Nitrogen Reduction to Ammonia at Low Overpotential in Aqueous Electrolyte under Ambient Conditions. *ChemSusChem*. **2018**, *11*, 3416-3422.
 - 19. Li, X.; Li, T.; Ma, Y.; Wei, Q.; Qiu, W.; Guo, H.; Shi, X.; Zhang, P.; Asiri, A. M.; Chen, L.; Tang, B.; Sun, X., Boosted Electrocatalytic N₂ Reduction to NH₃ by Defect-Rich MoS₂ Nanoflower. *Adv. Energy Mater.* **2018**, *8*, 1801357.
 - 20. Wang, H.; Wang, L.; Wang, Q.; Ye, S.; Sun, W.; Shao, Y.; Jiang, Z.; Qiao, Q.;

- Zhu, Y.; Song, P.; Li, D.; He, L.; Zhang, X.; Yuan, J.; Wu, T.; Ozin, G. A., Ambient Electrosynthesis of Ammonia: Electrode Porosity and Composition Engineering. *Angew. Chem. Int. Ed.* . **2018**, 57, 12360-12364.
21. Wang, X.; Wang, W.; Qiao, M.; Wu, G.; Chen, W.; Yuan, T.; Xu, Q.; Chen, M.; Zhang, Y.; Wang, X.; Wang, J.; Ge, J.; Hong, X.; Li, Y.; Wu, Y.; Li, Y., Atomically dispersed Au₁ catalyst towards efficient electrochemical synthesis of ammonia. *Sci. Bull.* **2018**, 63, 1246-1253.
22. Nazemi, M.; Panikkanvalappil, S. R.; El-Sayed, M. A., Enhancing the rate of electrochemical nitrogen reduction reaction for ammonia synthesis under ambient conditions using hollow gold nanocages. *Nano Energy*. **2018**, 49, 316-323.